13th World Conference on Earthquake Engineering
Vancouver, B.C., Canada
August 1-6, 2004
Paper No. 2398

AN ANALYSIS OF THE BEHAVIOR OF HYBRID STEEL BEAM – RC COLUMN CONNECTION

Jose C. ADAJAR[1], Toshiyuki KANAKUBO[2], Masahiro NONOGAMI[3], Nobuo KAYASHIMA[3], Yasuhisa SONOBE[4], Masami. FUJISAWA[5]

SUMMARY

A hybrid connection has been proposed to connect reinforced concrete columns and steel beams. Analytical and experimental studies have been conducted to investigate the performance of the proposed connection. The connection is designed to consist of welded plates that form an encasement to confine the concrete and the reinforcing bars. Results of analyses and experiments on loads, displacements, stresses and strains are presented to describe the general structural performance of the connection. Comparisons among specimens have been conducted to study the effects of parameter changes. Results indicate that the hybrid connection provides adequate strength and ductility.

INTRODUCTION

A hybrid framing design scheme has been considered to build a nine-story building in Japan. As illustrated in Fig. 1, the frame consists of steel beams that are connected to reinforced concrete (RC) columns. The beam-column connection is herein called the "hybrid connection". A particular design idea for the hybrid connection has been proposed.

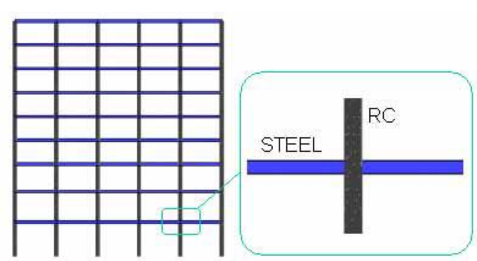

Figure 1. Framing System

As shown in Fig. 2, the connection consists of a welded steel plate encasement confining the concrete and the reinforcing bars. The encasement has openings that allow reinforcing bars to pass through the connection. A square tubing at the center of the encasement serves as the inner core confinement and

[1] Structural Engineer / Owner, AJIISS Engineering, Dallas, Texas, USA. Email: jadajar@ajiiss.com
[2] Professor, University of Tsukuba, Ibaraki, Japan. Email: kanakubo@kz.tsukuba.ac.jp
[3] Research Engineer, Daisue Construction Corporation, Osaka, Japan.
[4] Professor, Ashikaga Institute of Technology, Tochigi, Japan
[5] Professor, Tsukuba College of Technology, Ibaraki, Japan

the outer plates act as an outer confining reinforcement.

Objective
This research aims to study the behavior of the proposed hybrid connection through analytical and experimental investigations.

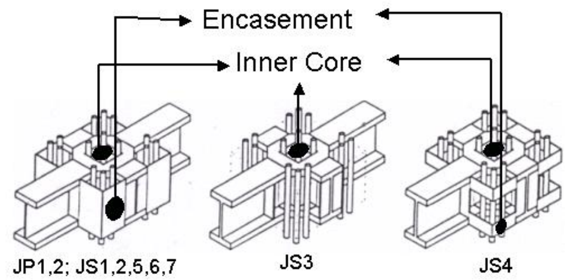

Figure 2. Beam-column connections.

ANALYTICAL INVESTIGATION

Basic Structural Macro Models

Preliminary calculations have been conducted using macro models to determine the approximate governing applied loads and material stresses. Considering the beam-column connection at the second floor of a nine-story building and the testing laboratory capabilities, the calculations were based on two model types that were classified according to mode of failure. The first model type, termed herein as "beam-yielding model", was for a failure mode governed by the steel beam. The second type, herein called "concrete-crushing model" was for a concrete compression failure mode. All model sizes are approximately one third of the actual structures. (Show two models with properties indicated.)

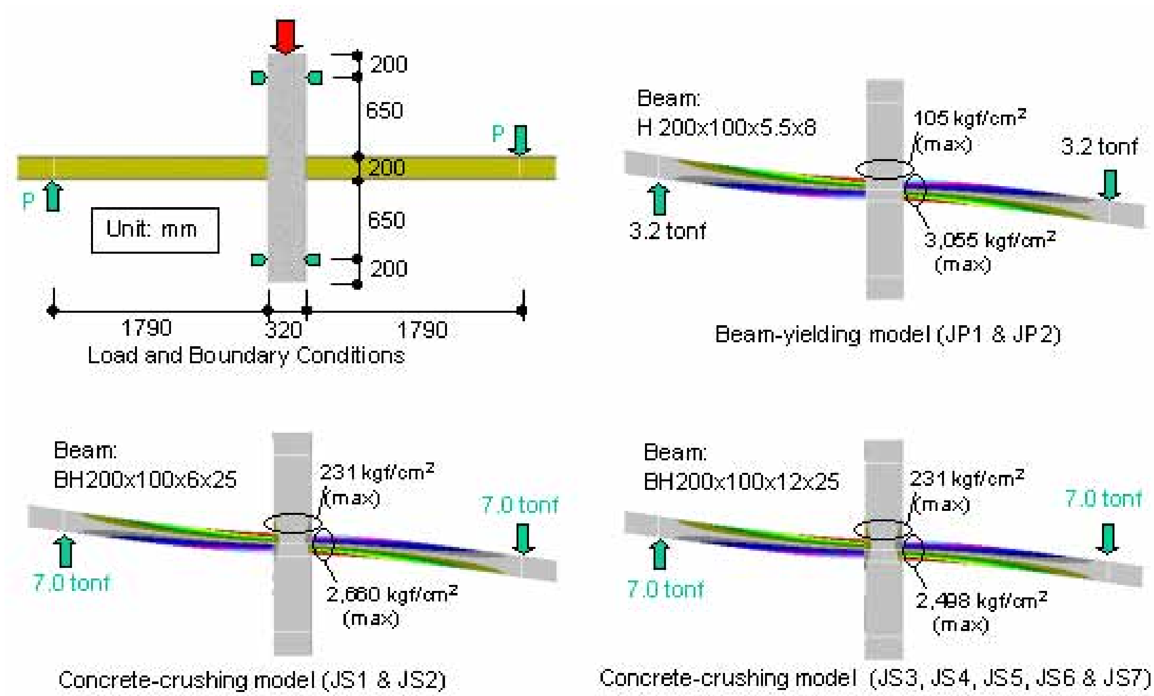

Figure 3. Preliminary analytical models.

Sizes and Material Properties
The lengths of the models for beams and columns are shown in Fig. 3. The beam sizes have been considered based on the commercially available steel sections. The column cross section is 320 mm x 320 mm. Beam size is 200 mm x 100 mm. The column/beam depth proportion Dc/Db is 1.6 and the width proportion Bc/Bb is 3.2. The sizes and material properties of the structural elements are as follows:

Beam-yielding model: A 320 mm x 320 mm concrete section was used for the column. The beam size was H 200 (depth in mm) x 100 (height) x 5.5 (web thickness) x 8 (flange thickness). A compressive strength of 400 kgf/cm^2 (5600 PSI) was assumed for concrete. The yield strength of beam was assumed to be 3000 kgf/cm^2 (42,700 PSI)

Concrete-crushing model: The size of the column was also 320 mm x 320 mm. Two sizes of beams, namely: BH 200 x 100 x 6 x 25 and BH 200 x 100 x 12 x 25, were used. The design compressive strength of concrete was assumed to be 200 kgf/cm^2 (2800 PSI). The yield strength of the beam was assumed to be 4000 kgf/cm^2 (57,000 PSI)

Loads and assumed Boundary Conditions
The bottom of the column was restrained to move upward or downward as shown in Fig. 3. Lateral restraints were placed at 200 mm from both ends of the column. An axial load was applied on top of each column. The additional stresses (Load/concrete section) on concrete due to axial loads were not presented in order to simplify the approximation. Beams were subjected to anti-symmetrical bending moments by applying loads at beam-ends.

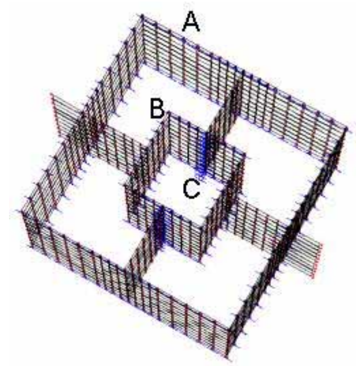

Figure 4. Boundary conditions.

Results of Preliminary Calculations
Using the sizes and material properties mentioned above, the beam-yielding model indicates that the steel beam yields when the applied load reaches approximately 3.2 tonf as shown in Fig. 3. In the vicinity of the hybrid connection, the maximum stress in the steel beam is 3,055 kgf/cm^2. The indicated maximum stress in concrete near the area of the connection is approximately 105 kgf/cm^2.

On the other hand, each concrete-crushing model indicates that concrete governs when the applied load is approximately 7.0 tonf. When the maximum stress in concrete is 231kgf/cm^2, the indicated highest stress level in beam BH200x100x6x25 is 2,660 kgf/cm^2. For beam BH200x100x12x25 with a thicker flange, the highest stress level is 2498 kgf/cm^2.

Steel Connector Micro Model Analyses
In order to study the flow of stresses from steel beams to steel connectors, micro models of designed specimens were created. Considering the interaction of the concrete column, a set of boundary conditions A, B, and C, as shown in Fig. 4, were assumed. Boundary conditions A and B indicate that the encasement perimeter and the inner tube are restrained to move upward or downward. Nodes in line with the middle of the tube are assumed to be pin-connected. The governing loads obtained in the preliminary calculations of the macro models were used to analyze the micro models. Using the properties of the designed experimental specimens, nine micro models were made as shown in Table 1.

Results of Micro Model Analyses

JP1 and JP2 Comparison
Figure 5 shows the stress results for beam-yielding model JP1 as compared to JP2. The properties of JP1 are the same as those of JP2 except that JP1 is cross-shaped with both beam ends loaded while JP2 is half-cross with only one beam end loaded. When the applied load at each beam end is 3.2 tonf, flanges of JP1 indicate a maximum stress of 6,931 kgf/cm^2 as compared to 7,077 kgf/cm^2 in JP2. Flanges that are just outside the connection encasement are within the assumed 3,000 kgf/cm^2 yield stress. However, the stresses on flanges inside the encasement are more than twice the yield strength particularly at corners where flanges change in shape.

The maximum stresses on JP1 and JP2 webs are 3,149 kgf/cm^2 and 3,097 kgf/cm^2 respectively. Connection encasements indicate stress levels of up to 504 kgf/cm^2 for JP1 and 470 kgf/cm^2 for JP2. The inner tube of JP1 shows a higher stress of 2,076 kgf/cm^2 as compared to only 1,997 kgf/cm^2 in JP2.

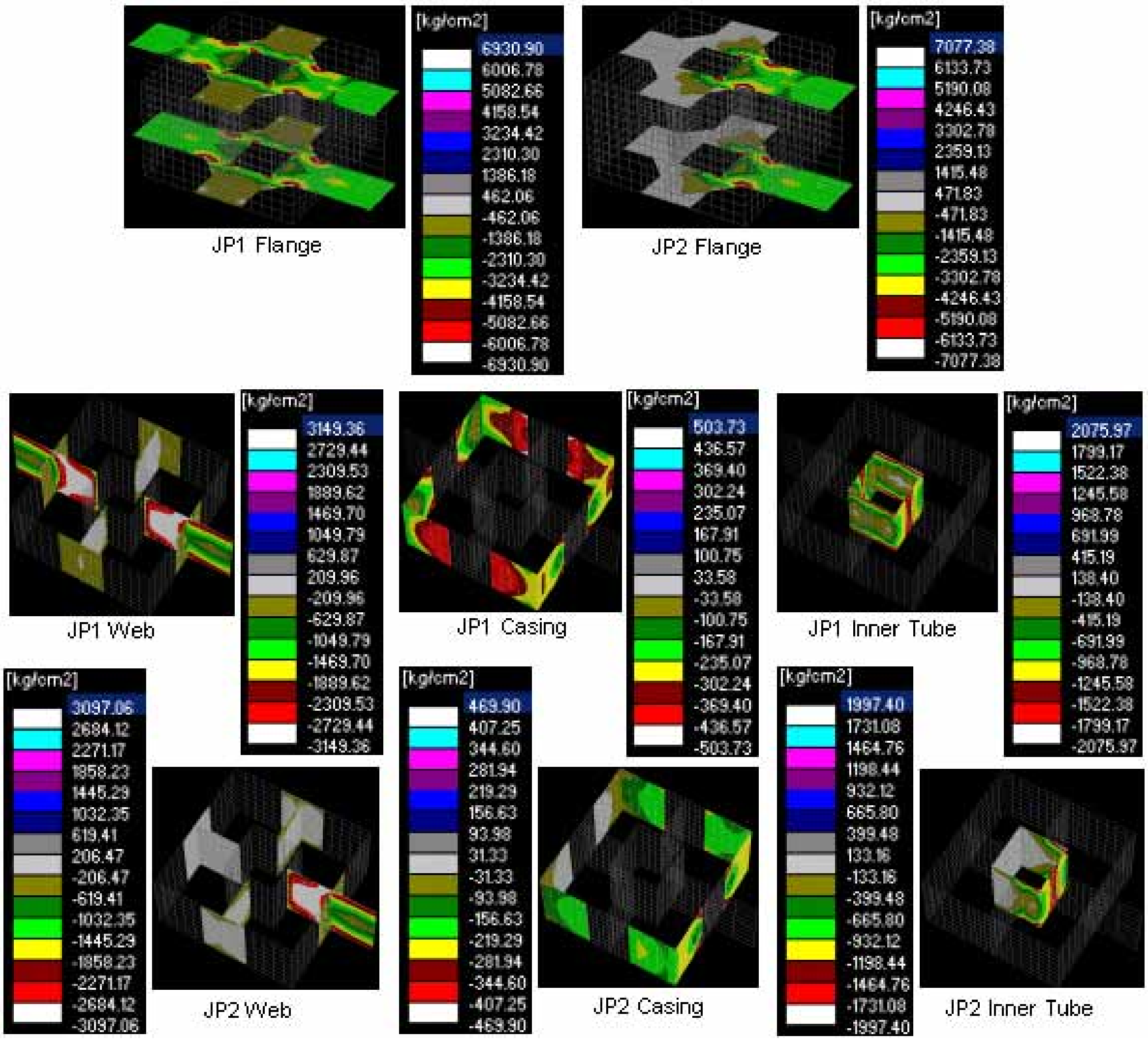

Figure 5. Stress results comparison for JP1 and JP2

JS1 and JS2 Comparison

The stress results of concrete-crushing model JS1 as compared to JS2 are shown in Fig. 6. JS1 and JS2 are identical except the encasement thickness that is 2.3 mm for JS1 and 4.5 mm for JS2. When the applied load at each beam end is 7.0 tonf, the maximum indicated stress on flanges of JS1 is 7,108 kgf/cm^2 as compared to 6,990 kgf/cm^2 in JS2. Flanges that are just outside the connection encasement are below the assumed 3,000 kgf/cm^2 yield stress. However, the stresses on flanges inside the encasement jump to more than twice the yield strength particularly at corners where flanges change in shape.

The maximum stresses on the webs of JS1 and JS2 webs are 3,064 kgf/cm^2 and 3,035 kgf/cm^2 respectively. Connection encasements indicate stress levels of up to 1180 kgf/cm^2 for JS1 and 1129 kgf/cm^2 for JS2. The inner tube of JS1 shows a higher stress of 2,768 kgf/cm^2 as compared to only 2,719 kgf/cm^2 in JS2.

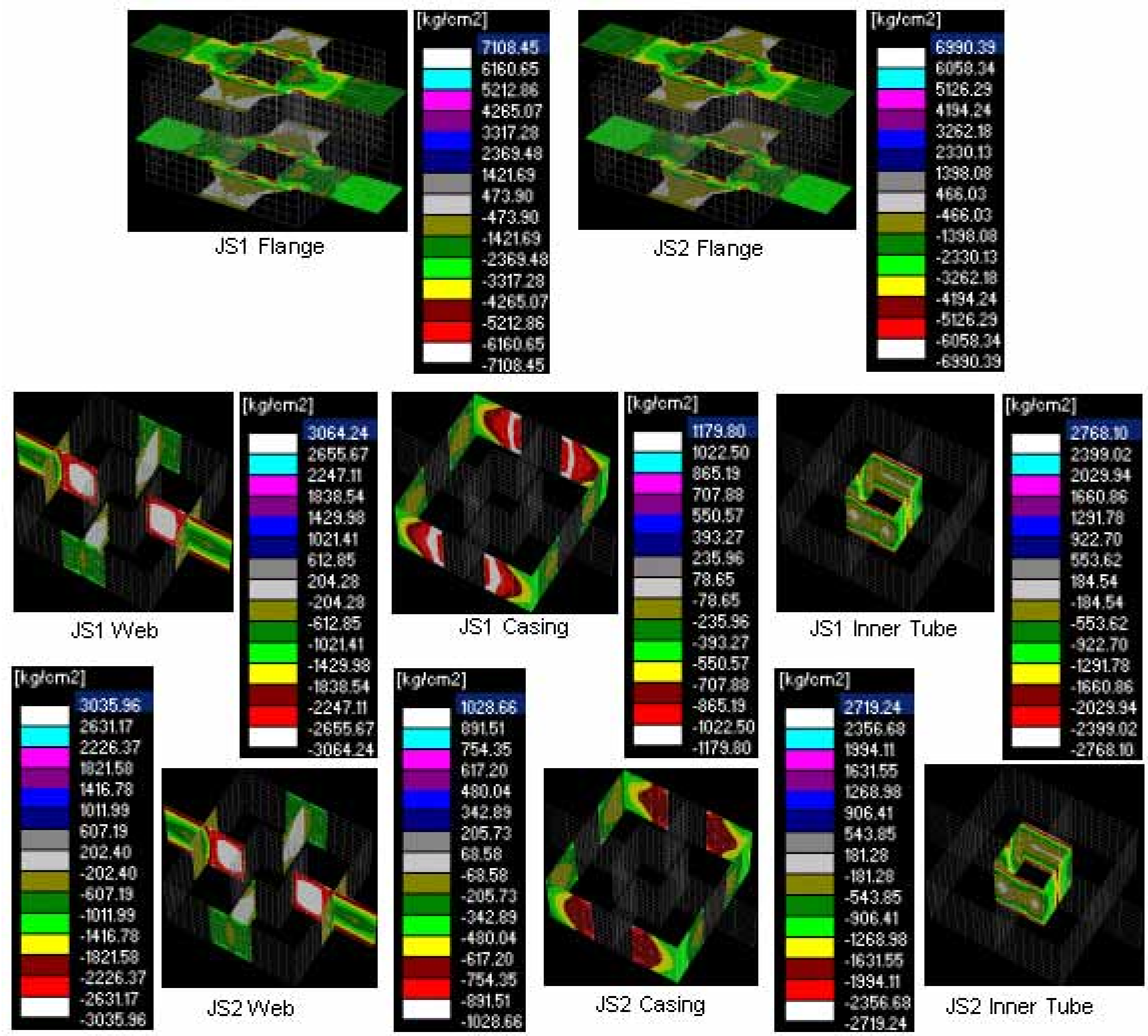

Figure 6. Stress results comparison for JS1 and JS2

JS3, JS4 and JS5 Comparison

JS3, JS4 and JS5 are concrete-crushing models that have the same properties except for an encasement thickness of 0.0 mm, 2.3 mm and 4.5 mm for JS3, JS4, and JS5, respectively. As shown in Fig. 7, when the applied load at each beam end is 7.0 tonf, the maximum indicated stress on flanges of JS3 is 5,611 kgf/cm^2 as compared to 5,404 kgf/cm^2 in JS4 and 5,322 kgf/cm^2 in JS5. As in other models that are mentioned above, flanges that are just outside the connection encasement are below the assumed 3,000 kgf/cm^2 yield stress. However, the stresses are more than double the yield strength on flanges inside the encasement where there are corners.

Figure 8 shows that the maximum stresses on the webs of JS3, JS4 and JS5 webs are 2,548 kgf/cm^2, 2,410 kgf/cm^2, and 2,481 kgf/cm^2 respectively. Model JS3 without encasement is compared to JS4 and JS5 with a maximum stress of 1018 kgf/cm^2 and 838 kgf/cm^2, respectively. The inner tube of JS3, JS4 and JS5 indicates a peak stress of 2,364 kgf/cm^2, 1,816 kgf/cm^2 and 2,217 kgf/cm^2, respectively.

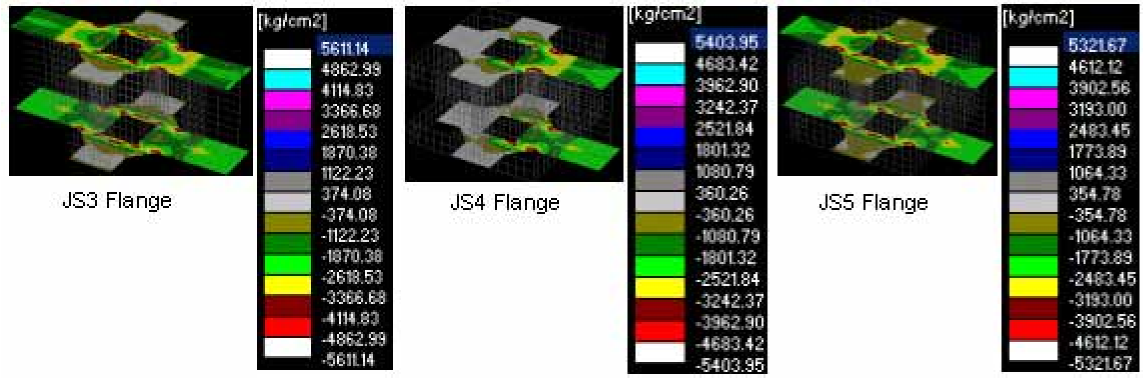

Figure 7. Stress results comparison for JS3, JS4 and JS5 flanges.

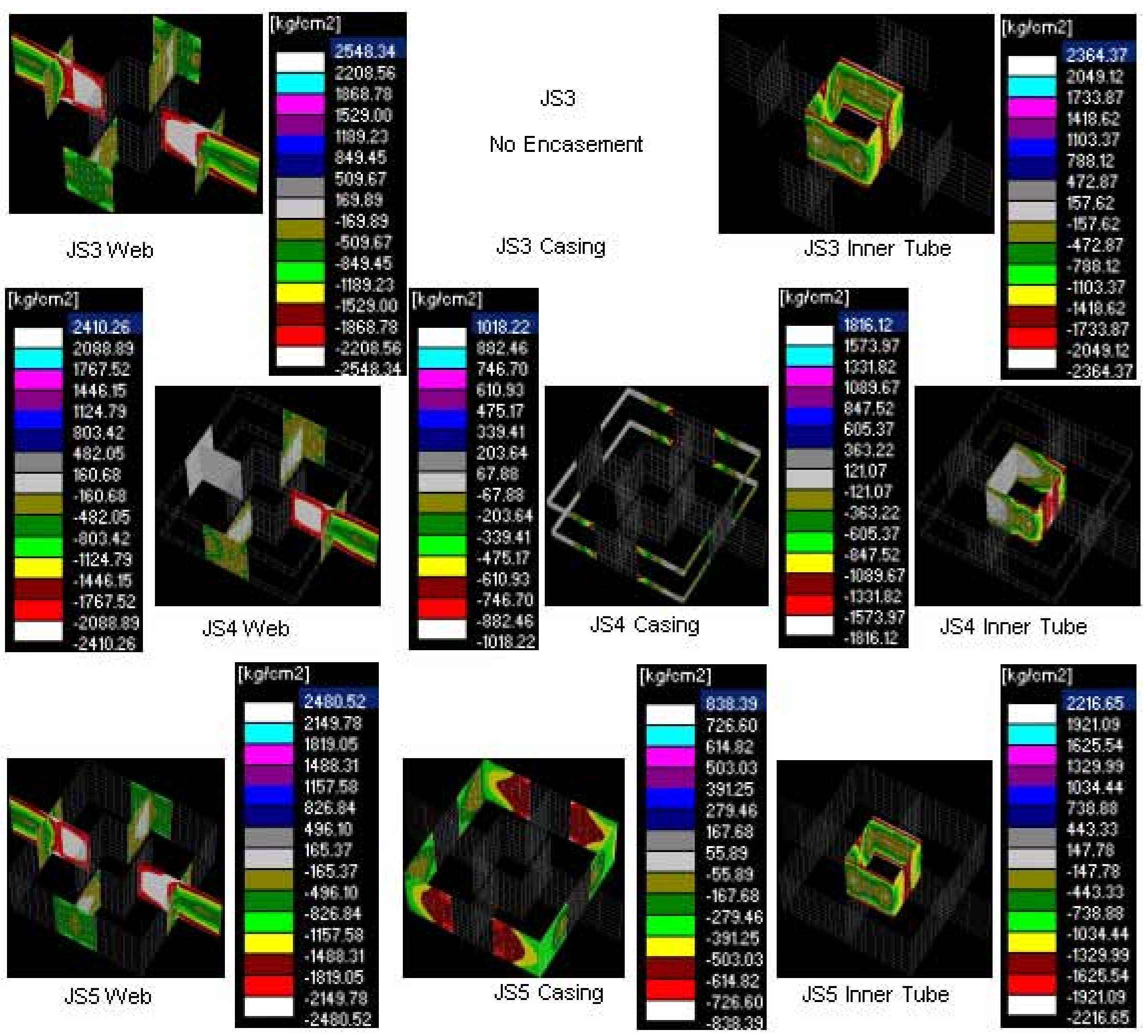

Figure 8. Stress results comparison for JS3, JS4 and JS5 components.

JS6 and JS7 Comparison
Figure 9 shows the stress results for concrete-crushing model JS6 as compared to JS7. The difference between the two models is the casing thickness. JS6 has 2.3 mm and JS7 has 4.5 mm. When the applied load at each beam end is 7.0 tonf, flanges of JS6 indicate a maximum stress of 6,843 kgf/cm^2 as compared to 6,731 kgf/cm^2 in JP2. Stresses on flanges that are just outside the connection encasement are below the assumed 3,000 kgf/cm^2 yield strength. The stress levels are consistent with the results of the macro model analysis. It is to be noted that the stress levels in some areas inside the encasement are more than twice the yield strength. Stress concentrations occur at plate corners where shapes change.

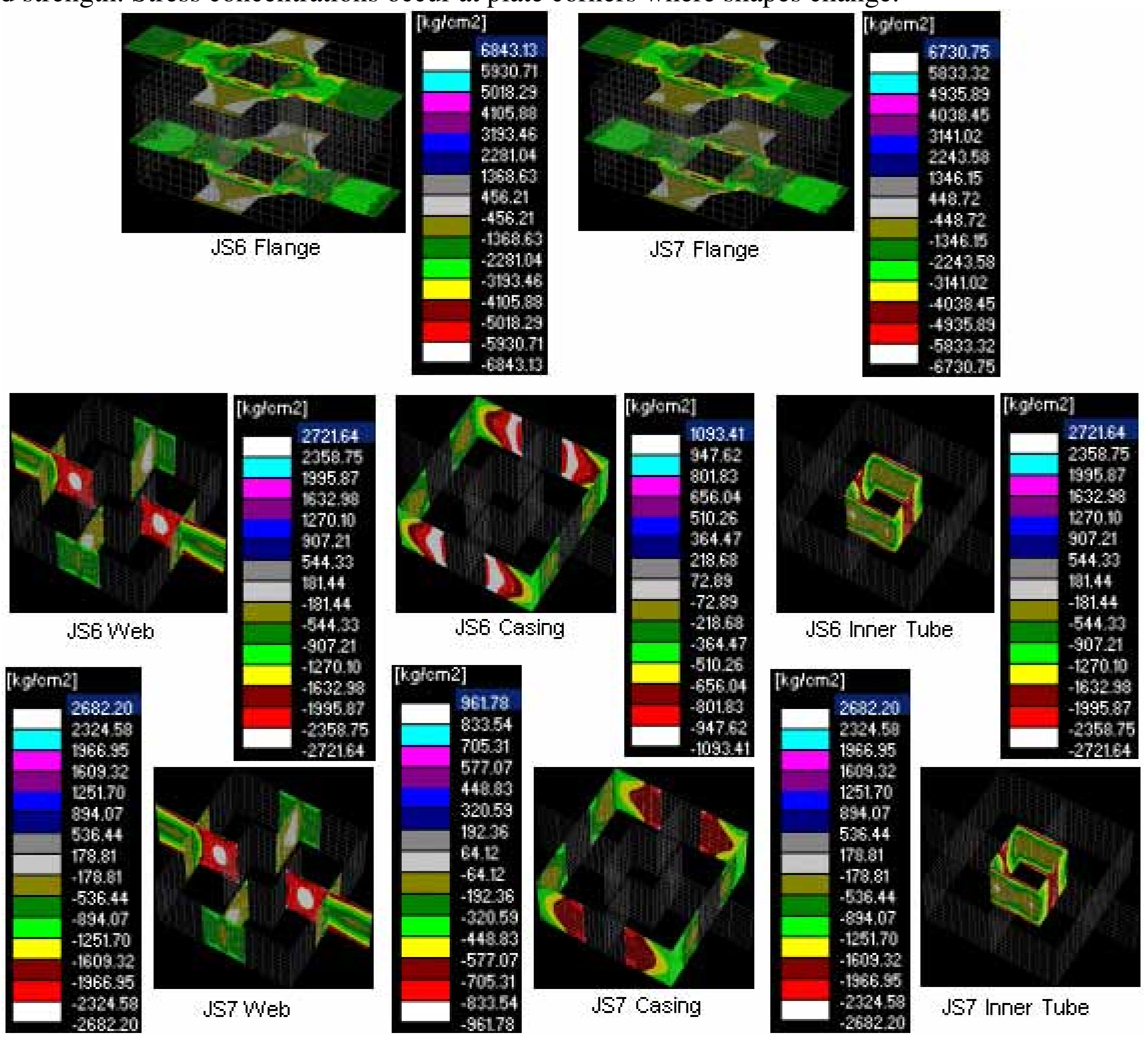

Figure 9. Stress results comparison for JS6 and JS7 components.

EXPERIMENTAL INVESTIGATION

Material Test Results

Table 2 shows the material test results. In JP1 and JP2, D13(SD345) (diameter=13mm; yield strength=345Mpa) reinforcing bars and high strength ties U5.1(SBPD1275/1420) were used for RC columns. The concrete strength was designed to be 360kgf/cm^2. H200x100x5.5x8 (SS400) was selected for the beams. In specimens JS1-JS7, D16(SD390) steel bars and high strength stirrups

U4.6(SBPD1275/1420) were utilized for columns. The design strength was 210kgf/cm^2 for concrete. Steel beams were BH200x100x6x25 (SM490) and BH200x100x12x25 (SM490).

Table 1. Properties of specimens.

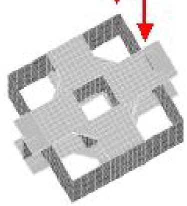

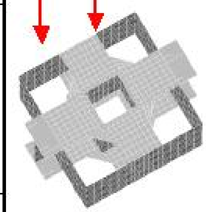

Specimen	JP1	JP2	JS1	JS2	
BxD(mm)	320x320				column
main bars	12-D13		12-D16		column
core bars	4-D13		4-D16		column
pg(%)	1.98		3.11		column
stirrups	4-U5.1@50		4-U6.4@50		column
pw(%)	0.50		0.75		column
DxBxt1xt2	H-200x100x5.5x8		BH-200x100x6x25		beam
inner tube	□ 120x120x6		□ 125x125x6		connx
outer plates	3.2		2.3	4.5	connx

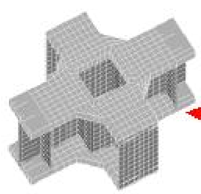

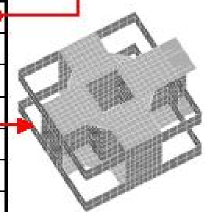

Specimen	JS3	JS4	JS5	JS6	JS7
BxD(mm)	320x320				
main bars	12-D16				
core bars	4-D16				
pg(%)	3.11				
stirrups	4-U6.4@50				
pw(%)	0.75				
DxBxt1xt2	BH-200x100x12x25				
inner tube	□ 125x125x9			□ 125x125x4.5	
outer plates	0.0	2.3	4.5	2.3	4.5

Table 2. Material test results.

Steel Plates				
plate properties	yield kgf/cm^2	ultimate kgf/cm^2	elongation %	part
SS400 t=2.3 mm	3610	4440	34	outer plate
SS400 t=4.5 mm	2900	3800	42	outer plate
SM490 t=6 mm	4030	5720	28	beam web
SM490 t=12 mm	3780	5550	28	beam web
SM490 t=25 mm	3500	5400	48	flange
SM490 t=28 mm	3650	5440	31	diaphragm
SM490 t=9 mm	3640	5320	28	steel tube
SN490 t=4.5 mm	4060	5620	34	steel tube
SN490 t=6 mm	4170	5650	32	steel tube

Steel Bars				
designation	yield kgf/cm^2	ultimate kgf/cm^2	elongation %	part
D13	3680	5510	26	main/core bars
D16	4820	6880	19	main/core bars
U6.4	13900	14900	9	stirrups

Concrete				
specimen	comp. strength kgf/cm^2	E kgf/cm^2 x10^{-5}	tensile strength kgf/cm^2	part
JP1	433	2.49		column
JP2	456	2.50		column
JS1	217	2.14	22.0	column
JS2	234	2.35	20.6	column
JS3	238	2.23	23.7	column
JS4	237	2.47	23.3	column
JS5	190	2.12	21.1	column
JS6	201	2.37	21.5	column
JS7	211	2.27	21.1	column

Loading Method and Sequence

As illustrated in Fig. 3, an oil jack was used to apply the axial load on the column, and actuators at beam-ends provided the antisymmetrical bending moments. The loading cycle and sequence, as shown in Fig.

10, started from a drift angle R=±1/800 and ended at R=±1/25. The drift angle was doubled after every two loading cycles. At R=±1/25, the cycle was done only once.

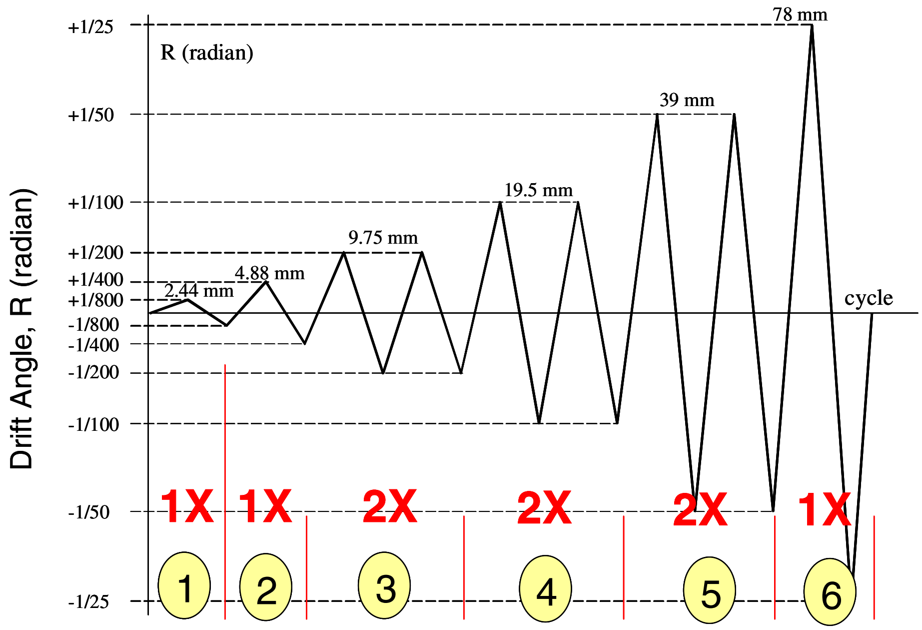

Figure 10. Loading cycle and sequence.

Displacement and Strain Gauges

Figure 11 shows the setup to measure relative displacements and curvatures in beams and column. Gauges to record shear deformations within the beam-column connection are shown in Fig. 12. Strain gauges placed at preferred locations to monitor strains on steel plates are shown in Fig. 13.

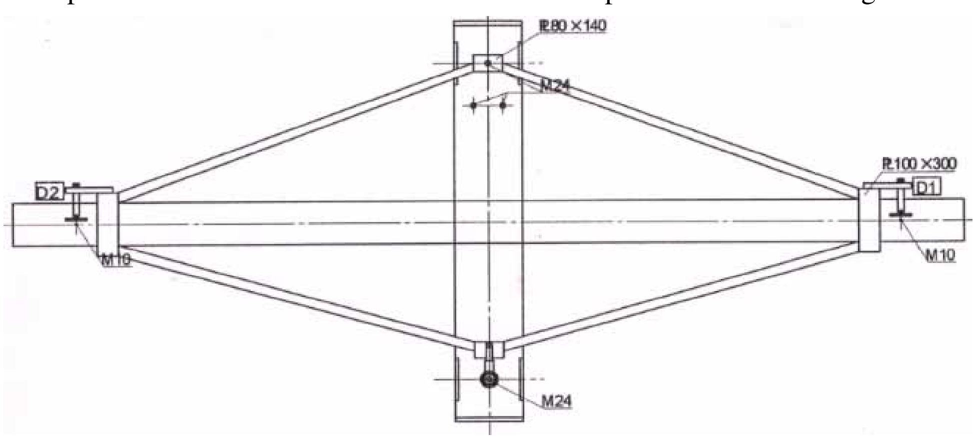

Figure 11. Setup of displacement gauges.

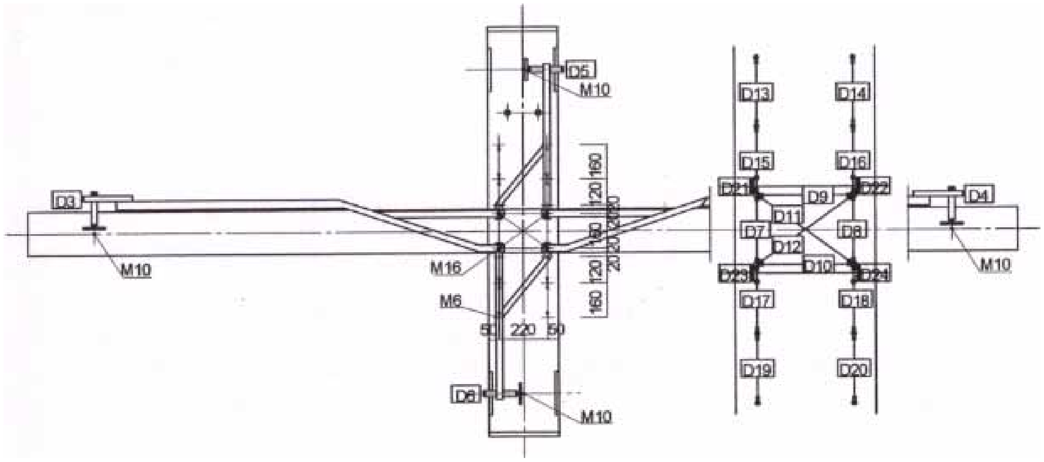

Figure 12. Shear deformation gauges.

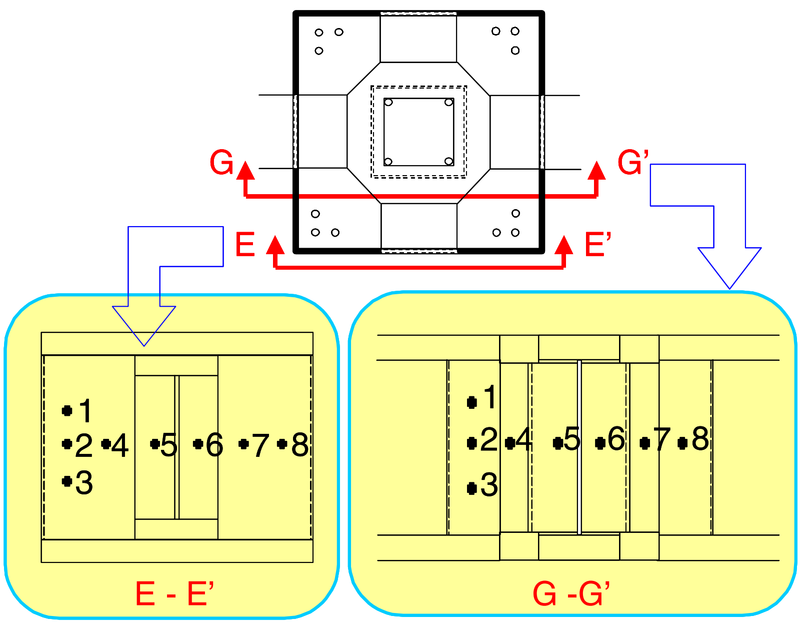

Figure 13. Strain gauges on steel plates.

TEST RESULTS

Loads, Displacements, Cracking, and Yielding

Load-displacement diagrams are shown in Figure 14. In specimens JP1 (cross shape) and JP2 (half cross shape), the maximum loads for both specimens are 4.2 tonf during the positive cycle and 4.4 tonf during the negative cycle. More visible cracks occurred in the column of half-cross specimen JP2 than in JP1. Cracks in JP1 are very minimal and occurred only near the beam-column connection. There was no indication of yielding in the steel reinforcements of the column. However, the web of the beam was yielding. In specimen JS1 that has steel encasement around the beam-column connection, cracks due to bending occurred in the column during a drift R=1/100 cycle. During this cycle, the end of the steel beam and some parts inside the beam-column connection were yielding. Encasement plates yielded during the last cycle when R=1/25. Shear cracks on the column was seen during R=1/25 cycle. A maximum load of 8.1 tonf was reached during this cycle. The maximum load was still less than the ultimate flexural strength of the column. In specimen JS3, where outer plate encasement was not present, the flexural cracks in the column occurred when R=1/200. During this cycle, shear and flexural cracks were noticed at the beam-column connection. Yielding of steel plates inside the beam-column connection and at beam-ends occurred during R=1/100. A maximum load of 6.2 tonf was attained at R=1/25. The ultimate flexural strength of specimen JS3 was not reached. In specimen JS4, flexural cracks started to occur when R=1/200. The beam started to yield upon reaching R=1/100. Plates inside the beam-column connection began yielding during R=1/50. In this cycle, shear cracks appeared in the area of beam-column connection. A maximum load of 11.1 tonf was reached when R=+1/25. This maximum load was almost equal to the beam ultimate bending capacity.

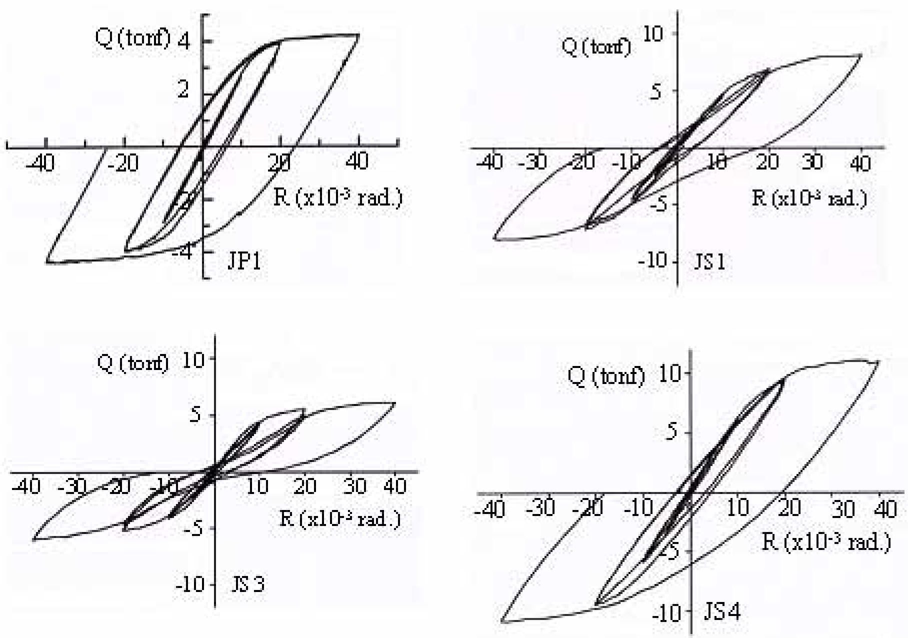

Figure 14. Load – displacement diagrams.

Strain Distributions

The maximum indicated strain in the square tubing is 900μ for cross shape specimen JP1 and 400μ for half cross shape specimen JP2. The outer plates of the beam-column connection indicated a maximum strain of 500μfor JP1 and 300μfor JP2. Figure 15 shows the strain values on the plates inside the connection when R=1/25. Strain

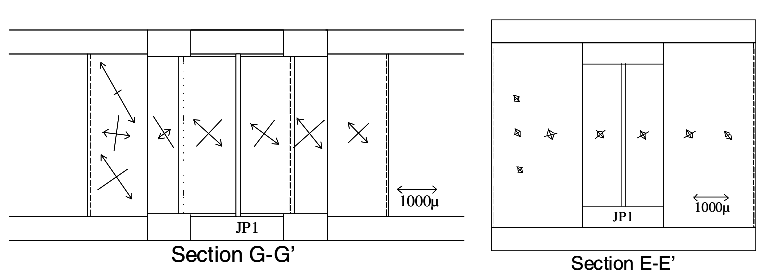

Figure 15. Typical strain values in beam-yielding type specimens.

readings for specimens JS1, JS3 and JS4 when R=1/25 are plotted in Fig. 16. The maximum load was designed to be governed by the beam-column connection. This was true for specimens JS1 and JS3 where the inner plates and square tubing indicated large strains. However, in JS4, the specimen that was designed to fail in bending at beam-ends, relatively small strains on the square tube were observed. Although strains on the outer plates of JS1 were smaller than those on the square tubing, yielding occurred on the outer plates.

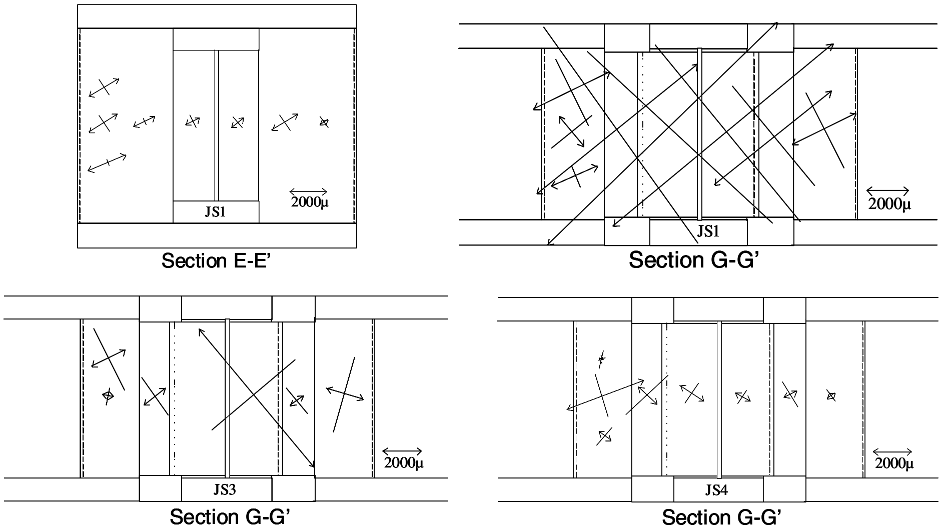

Figure 16. Typical strain values in concrete-crushing type specimens.

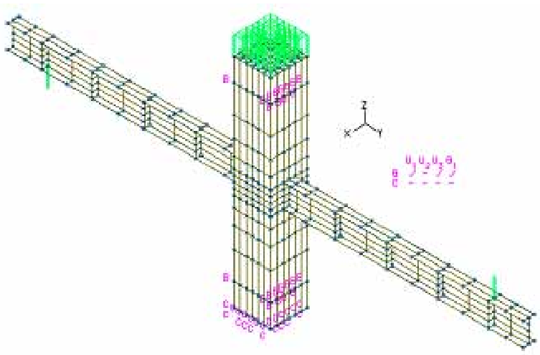

Figure 17. Load and boundary conditions.

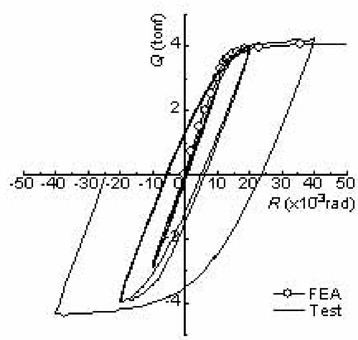

Figure 18. Analytical and experimental Load –displacement relations for JP1.

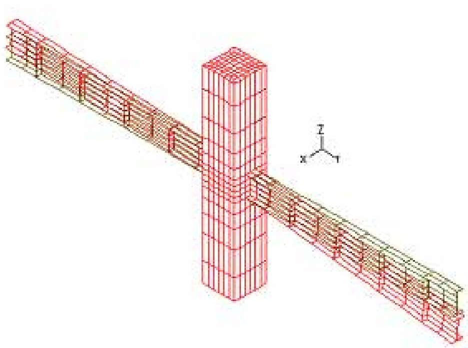

Figure 19. Analytical deflection of JP1.

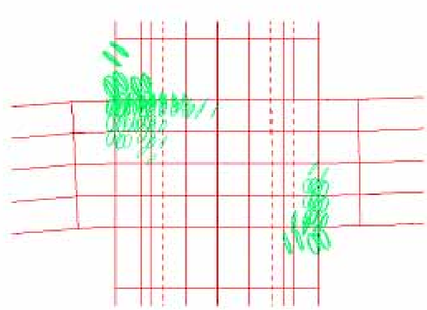

Figure 20. Theoretical Crack formations in JP1

Results of Hybrid Connection Analytical Investigation

A structural model was created using ADINA finite element analysis program to simulate the behavior of a specimen JP1. The model indicating the load and boundary conditions is shown in Fig. 17. Full fixity was assumed at the bottom end of the column. It was also assumed that there was no translation along y-axis at intermediate points near the top and bottom ends of the column where confining oil jacks were located. The model consisted of 2-node line elements for steel reinforcing bars, 4-node shell elements for steel plates, and 8-node solid elements for concrete for a total of 1340 nodes. Bilinear model with Von Mises yield condition was used for steel elements. Figure 18 shows that the experimental and theoretical load-displacement relations for the beam of specimen JP1 are in good agreement. Both analytical and experimental investigations indicated that when R=1/25, the deflection of the beam is about 95% of the total deformation of the specimen as can be observed in Fig. 19. During testing, cracks were observed on the surface of the column in the area of the beam-column connection but analytical results indicated that cracks formed beneath the surface as shown in Fig. 20. Theoretical results for stresses on plates inside the connection were notably different from the experimental results. A response model for bond between concrete and steel plates was not provided. This may account for the difference between analytical and actual stress results in the inner part of the connection.

CONCLUSIONS

It can be concluded that the proposed design for the hybrid beam-column connection provides an adequate strength and ductility when the encasement is present. The additional resistance due to confinement of concrete enhances the capacity of the connection. The hybrid connection method can be an alternative design in building frame type structures. Design estimates can be made using finite element analytical model of the steel beam and steel plates in the beam-column connection with the reinforced concrete column action assumed as the boundary supports. The shear strength range of the connection can be calculated using Sakaguchi equation. Further investigation of the connection performance considering the bond between steel and concrete is recommended.